URSI GASS 2021, Rome, Italy, 28 August - 4 September 2021

Half-Mode Substrate Integrated Waveguide Leaky-Wave Antenna Based on a Dielectric Layer with Periodic Perforations

Kamil Yavuz Kapusuz*, Andres Vanden Berghe, Sam Lemey, and Hendrik Rogier
Department of Information Technology, IDLab/Electromagnetics Group, Ghent University/IMEC,
Technologiepark-Zwijnaarde 126, 9052 Ghent, Belgium

Abstract

A low-cost multilayer antenna is proposed for the next-generation automotive radar systems at millimeter waves. The antenna consists of a multilayer half-mode substrate integrated waveguide (HM-SIW) leaky-wave antenna (LWA) based on a dielectric layer with periodic perforations. Its stack-up consists of a 0.5-mm-thick Rogers 4350B substrate and two 1.0-mm-thick FR4 substrates assembled by 1.4-mm-diameter alignment pins and fixations. Measurements of a 126-mm-long fabricated prototype revealed a -10-dB impedance bandwidth of 6.9 GHz, covering the 22 GHz to 28.9 GHz band. The measured gain equals 15.5 dBi at 24 GHz, resulting in a total efficiency of more than 85%. Moreover, the measured radiation patterns in the [22-26] GHz band exhibit an average 3-dB beamwidth of 11.5^o and sidelobe levels (SLL) better than 20 dB up to a scan angle of 20^o.

1 Introduction

To reduce risky and dangerous behavior on the roads, autonomous vehicles gain increasingly more interest. They rely on diverse technologies such as innovative sensors and actuators, sophisticated algorithms and powerful processors [1]. In particular, there is a high demand for innovative sensors and actuators providing size and weight reduction, while generating stable high-gain steerable beams [2]. Moreover, these sensors should exhibit high integrability and low loss at a reduced cost compared to their current counterparts [3]. Furthermore, to avoid costly post-process tuning steps and, consequently, meet the projected high-volume market demands, the foreseen systems require rapid synthesis, meeting stringent specifications with high robustness to manufacturing tolerances [4].

Substrate integrated waveguide (SIW) leaky-wave antennas (LWAs) are excellent candidates for automotive radar technology as they implement frequency-scanned directive beams using low profile topologies that are easily integrated into the readily available surfaces of vehicles [5]. In addition, they combine efficient shielding with simple and cost-effective manufacturing [6]. Furthermore, dedicated topologies can improve the compactness of the antennas [7]. Despite these benefits, conventional dielectric-filled SIW LWAs inevitably limit radiation efficiency, making them less suited for commercial automotive radar, targeting highly efficient antenna systems in a small form factor [8].

To reach an optimum in terms of antenna performance and manufacturing cost, SIW LWAs based on periodic perforations of the dielectric substrate were studied in [9, 10]. [9] presents an LWA based on substrate integrated nonradiative dielectric (SINRD) waveguide technology at 96 GHz, while [10] proposes a double-sided LWA using the substrate integrated slab waveguide (SISW) at 28 GHz. Although these topologies provide good antenna performance, they suffer from a large size.

This paper presents a new half-mode SIW (HM-SIW) LWA, based on periodic perforations of the dielectric substrate, creating air holes. A half-mode implementation of an LWA is leveraged to realize a compact antenna covering the [22--26] GHz frequency band. Exploiting air as a low-loss medium, the periodic holes control the phase and leakage constant in the highly-efficient HM-SIW LWA. The developed antenna is suitable for easy installation on vehicles for automotive radar applications.

2 HM-SIW LWA Topology and Operation Principle

Fig. 1(a) shows the layout of the developed HM-SIW LWA topology based on a dielectric layer with periodic perforations [8]. The developed antenna consists of one layer of high-performance dielectric substrate (Layer 2) and two low-cost layers (Layer 1 and Layer 3). Layers 1 and 3 provide support to the top and bottom conducting boundaries of the HM-SIW. They sandwich the middle dielectric substrate (Layer 2), periodically perforated by an array of air-holes.

To implement an effective broadband interconnection to the antenna, in a first step, a three-sections' transition is created from the SMA probe to the half-mode LWA [Fig. 1(b)], inspired by an SIW transition on a high-to-low dielectric constant substrate introduced in [11]. The triangular-shaped di-

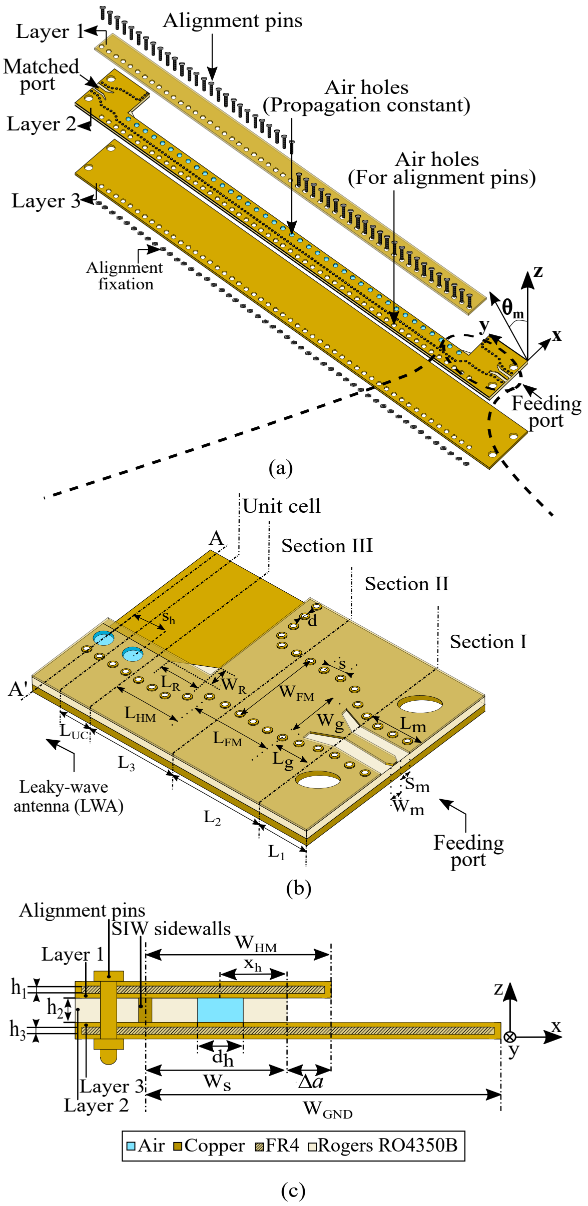

Figure 1. Concept and architecture of the HM-SIW LWA based on a dielectric layer with periodic perforations. (a) Exploded view. (b) Three-sections' transition from feeding point probe to HM-SIW LWA. (c) Cross-sectional view at AA'. Optimized dimensions: W_m = 1 mm, S_m = 0.5 mm, L_m = 3.34 mm, W_g = 3.22 mm, L_g = 1.4 mm, W_{FM} = 4.42 mm, L_{FM} = 53.9 mm, W_s = 1.9 mm, L_{HM} = 3.7 mm, W_R = 1.32 mm, L_R= 2.83 mm, L_T = 11.24 mm, L_{UC} = 1.3 mm, Δa = 0.7 mm, W_{GND} = 10.5 mm, d_h = 1.1 mm, s_h = 1.3 mm, x_h = 0.9 mm, d = 0.4 mm, s = 0.8 mm, h_1 = h_3 = 1 mm, h_2 = 0.5 mm.

electric substrate [Fig. 1(b)] tapers from a full-mode dielectric SIW into the HM-SIW LWA based on a dielectric layer with periodic perforations. This small periodically perforated dielectric supporting region inside the HM-SIW LWA is preserved to guarantee sufficient mechanical strength and to control the complex propagation constant of the leaky-wave modes propagating along the longitudinal direction. Then, to obtain a high antenna efficiency in a short antenna, the air-filled region is judiciously designed in Layer 2 to minimize the dielectric loss of the material. Finally, all layers are assembled by 1.4-mm diameter alignment pins and fixations, to guarantee sufficient electrical contact and to provide accurate alignment.

This topology is optimized to generate a highly directive and steerable beam over a broad scan range. Therefore, the HM-SIW cross section is implemented by cutting the SIW waveguide in half and extending Layer 3 at the open aperture side [Fig. 1(c)]. Subsequently, radiation is achieved by using a dominant slow-wave non-radiative SIW mode that excites a fast higher-order (n = -1) space wave [12]. This is accomplished by introducing a periodic structure along the length of the open waveguide. Consequently, a highly-directive fan beam in the yz-plane with frequency scanning is obtained.

3 Effects of Periodic Perforation on Radiation Characteristics

To determine the optimum perturbation parameters for constructive interference along the different scan angles, a parametric study was performed. A summary of the antenna dimensions used in this design is presented in Fig. 1.

3.1 Total Antenna Efficiency

Fig. 2 illustrates the total antenna efficiency curves for different air hole dimensions. Note that the air hole diameter controls the total antenna efficiency. On the one hand, the amount of air in the configuration mainly determines the antenna efficiency; an increase in air hole diameter (d_h) boosts the total antenna efficiency, as seen in Fig. 2(a). In contrast, an increase in the air hole spacing (s_h) decreases the total antenna efficiency, as demonstrated by Fig. 2(b). Similarly, the total antenna efficiency decreases when the offset (x_h) at the open side increases, as depicted in Fig. 2(c).

3.2 Beam Direction and Scanning Range

The beam direction and scanning range for different air hole parameters are illustrated in Fig. 3 and Fig. 4. As seen in Fig. 3, the air hole parameters control the beam direction within the targeted frequency band. If the diameter of the air holes (d_h) increases or the center-to-center spacing (s_h) between air holes decreases, the beam moves closer to broadside [Fig. 3(a) and Fig. 3(b)]. In addition, an increase in the offset (x_h) of the air holes from the open side up to 0.4 mm moves the beam closer to broadside while the beam direction moves away from broadside when the air holes are positioned further from the open side [Fig. 3(c)]. However, the scanning range remains in the order of 20°.

An additional parameter study assesses the effects of the dielectric width (w_s) over the upper conductor width (W_{HM}) ratio on the scanning range performance. Fig. 4 depicts the relation between the dielectric width (w_s) over the upper

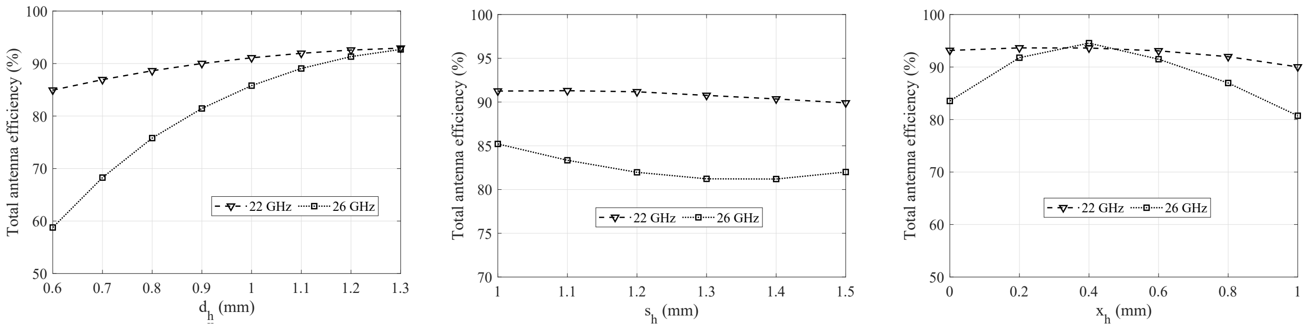

(a) (b) (c)

Figure 2. Influence of the air hole parameters on the total antenna efficiency. Variations of (a) d_h, (b) s_h and (c) x_h.

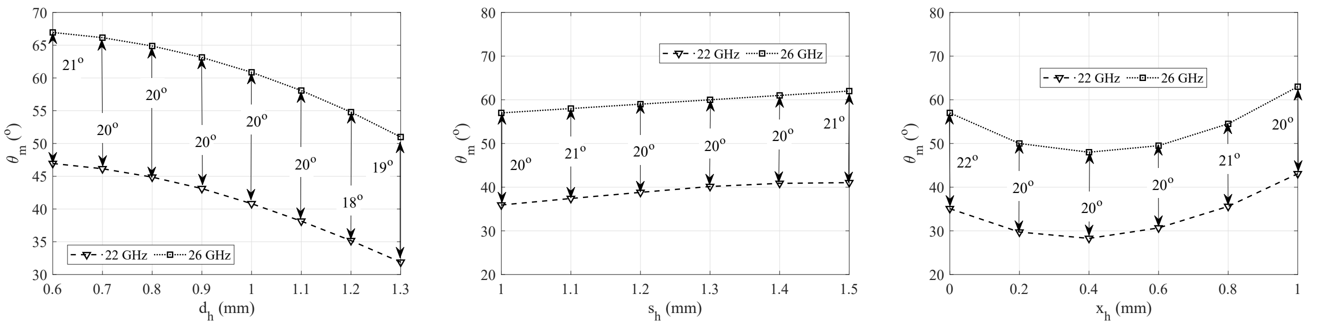

(a) (b) (c)

Figure 3. Influence of the air hole parameters on the beam direction (θ_m) and scanning range. Variations of (a) d_h, (b) s_h and (c) x_h.

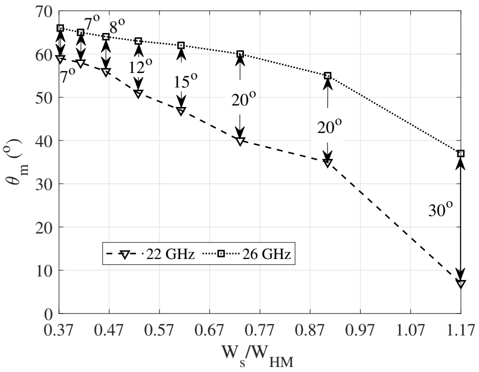

Figure 4. Influence of the dielectric width (w_s) over the upper conductor width (W_{HM}) ratio on the beam direction (θ_m) and scanning range.

conductor width (W_{HM}) ratio, w_s/W_{HM}, and the scanning range. A wider dielectric width enables to scan over a larger range of angles for the same frequency range.

4 Prototype and Experimental Results

As a proof-of-concept, an LWA prototype has been built and measured. 77 holes were perforated to reduce the surface wave at the matched port to less than 20%, achieving an 80% leaky-wave end point efficiency according to CST simulations. Photos of the prototype before and after final assembly are shown in Fig. 5(a) and (b), respectively. Its dimensions are 126 x 10.5 mm^2 (without connectors) while the panel size on which the antenna is built equals 126 x 15 mm^2. The antenna exhibits and extremely low profile, being $h_{antenna} = h_1 + h_2 + h_3 = 2.5$ mm.

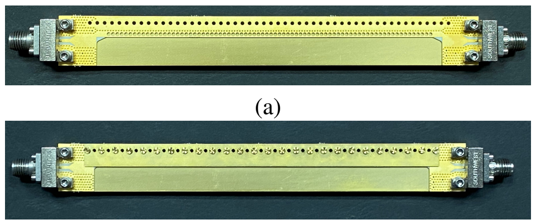

(b)

Figure 5. Fabricated prototype. (a) Layer 2 assembled with Layer 3 before adding Layer 1. (b) Top view after final assembly.

The S-parameters are measured with an Agilent E8364B PNA Microwave Network Analyzer, calibrated with a short-open-thru-load (SOTL) kit. The far-field radiation patterns are characterized in an anechoic chamber by an NSI-MI spherical near-field antenna measurement system and a Keysight N5242A PNA-X VNA through gain comparison with an ANT-SGH-22-33 standard gain horn antenna. A model of the solder-free K-type (2.92 mm) End-Launch connectors by Southwest Microwave is included in the simulations for adequate comparison between measured and simulated performance of the antenna.

The measured and simulated S-parameters are shown in Fig. 6. The measured reflection coefficient has a -10 dB bandwidth in the range 22 GHz to 28.9 GHz, with a measured impedance bandwidth of 6.9 GHz. The small difference between simulations and measurements is due to the tolerances of the fabrication process and of the RF material exploited in Layer 2.

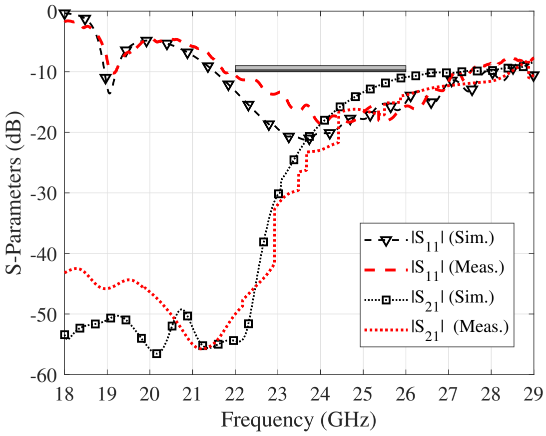

Figure 6. Measured and simulated S-parameters.

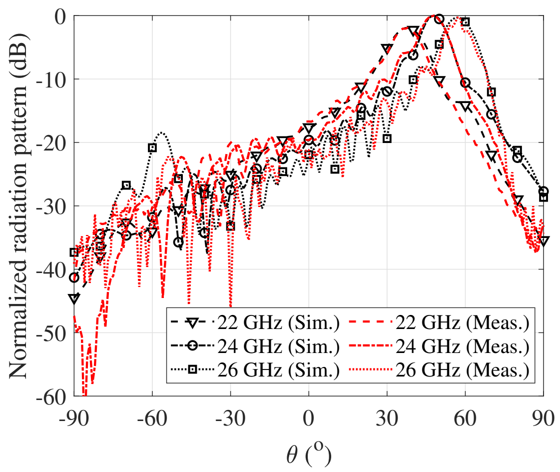

Figure 7. Radiation patterns in the *yz*-plane.

The simulated and measured *yz*-plane radiation patterns for the antenna in the [22–26] GHz frequency band are shown in Fig. 7. A good agreement between simulations and measurements is found. The typical frequency scanning behavior from 38^o to 58^o is shown in the *yz*-plane patterns. A realized gain of 13.7 dBi, 15.5 dBi, and 15.7 dBi is found at 22 GHz, 24 GHz and 26 GHz, respectively. An average 3-dB beamwidth of about 11.5^o in the *yz*-plane is obtained, while maintaining a measured total antenna efficiency higher than 85% at 24 GHz. In the [22–26] GHz band, the sidelobe level (SLL) is better than 19 dB for the z>0 hemisphere. Finally, the cross-polarization ratio [defined as the ratio of the co-polarization gain to the cross-polarization gain] at 24 GHz equals 22 dB.

5 Conclusion

A novel low-profile antenna for 24-GHz band automotive radars has been developed and experimentally characterized. A measured total efficiency higher than 80% was obtained. The very promising radiation performance, high efficiency and low cost make the proposed antenna a very good candidate for the next generation of automotive radars.

References

[1] Google autonomous car, (2020). [Online]. Available: https://waymo.com/

[2] W. Menzel and A. Moebius, "Antenna concepts for millimeter-wave automotive radar sensors," *Proc. of the IEEE*, **100**, 7, July 2012, pp. 2372–2379.

[3] I. Gresham *et al.* "A compact manufacturable 76-77-GHz radar module for commercial ACC applications," *IEEE Trans. Microw. Theory Tech.*, **49**, 1, Jan. 2001, pp. 44–58.

[4] J. Hasch *et al.* "Millimeter-wave technology for automotive radar sensors in the 77 GHz frequency band," *IEEE Trans. Microw. Theory Tech.*, **60**, 3, March 2012, pp. 845–860.

[5] J. Xu, W. Hong, H. Tang, Z. Kuai, and K. Wu, "Half-mode substrate integrated waveguide (HMSIW) leaky-wave antenna for millimeter-wave applications," *IEEE Antennas and Wireless Propag. Lett.*, **7**, 2008, pp. 85–88.

[6] J. Liu, D.R. Jackson, and Y. Long, "Substrate integrated waveguide (SIW) leaky-wave antenna with transverse slots," *IEEE Trans. Antennas Propag.*, **60**, 1, Jan. 2001, pp. 20–29.

[7] Y. Dong and T. Itoh, "Composite right/left-handed substrate integrated waveguide and half mode substrate integrated waveguide leaky-wave structures," *IEEE Trans. Antennas Propag.*, **59**, 3, March 2010, pp. 767–775.

[8] K.Y. Kapusuz, A. Vanden Berghe, S. Lemey, and H. Rogier, "Partially-filled half-mode substrate integrated waveguide leaky-wave antenna for 24-GHz automotive radar," *IEEE Antennas and Wireless Propag. Lett.*, **20**, 1, Jan. 2021, pp. 33–37.

[9] P. Mondal, and K. Wu, "A leaky-wave antenna using periodic dielectric perforation for millimeter-wave applications," *IEEE Trans. Antennas Propag.*, **64**, 12, Dec. 2016, pp. 5492–5495.

[10] E. Massoni, M. Bozzi, and K. Wu, "Increasing efficiency of leaky-wave antenna by using substrate integrated slab waveguide," *IEEE Antennas and Wireless Propag. Lett.*, **18**, 8, Aug. 2019, pp. 1596–1600.

[11] N. Ghassemi, I. Boudreau, D. Deslandes, and K. Wu, "Millimeter-wave broadband transition of substrate integrated waveguide on high-to-low dielectric constant substrates," *IEEE Trans. Compon., Packag. Manufact. Tech.*, **3**, 10, Oct. 2013, pp. 1764–1770.

[12] W. Rotman and A. Oliner, "Periodic structures in trough waveguide," *IRE Trans. Microw. Theory Tech.*, **7**, 1, Jan. 1959, pp. 134–142.